

Field-Dependent Critical Current in Type-II Superconducting Strips: Combined Effect of Bulk Pinning and Geometrical Edge Barrier

Andrey A. Elistratov, Denis Yu. Vodolazov, Igor L. Maksimov and John R. Clem*

Nizhny Novgorod University, 603600 Nizhny Novgorod, Russia

**Ames Laboratory and Department of Physics and Astronomy, Iowa State University, Ames, Iowa 50011-3160, USA*
(October 25, 2018)

Recent theoretical and experimental research on low-bulk-pinning superconducting strips has revealed striking dome-like magnetic-field distributions due to geometrical edge barriers. The observed magnetic-flux profiles differ strongly from those in strips in which bulk pinning is dominant. In this paper we theoretically describe the current and field distributions of a superconducting strip under the combined influence of both a geometrical edge barrier and bulk pinning at the strip's critical current I_c , where a longitudinal voltage first appears. We calculate I_c and find its dependence upon a perpendicular applied magnetic field H_a . The behavior is governed by a parameter p , defined as the ratio of the bulk-pinning critical current I_p to the geometrical-barrier critical current I_{s0} . We find that when $p > 2/\pi$ and I_p is field-independent, I_c vs H_a exhibits a plateau for small H_a , followed by the dependence $I_c - I_p \propto H_a^{-1}$ in higher magnetic fields.

The combination of a geometrical edge barrier and bulk pinning recently has been shown to strongly affect the properties of low-dimensional superconductors (thin films, single crystals, and tapes with high demagnetizing factors) placed in either a perpendicular magnetic field¹⁻⁵ or a transport-current-carrying state⁶⁻⁹. While most experimental studies of the field dependence of the critical current I_c are being interpreted solely on the basis of bulk-pinning theory (see for example¹⁰⁻¹⁴), a number of works^{6,8,15,16} have shown that a geometrical edge barrier (or surface barrier) may strongly affect I_c . In this paper we study the combined effect of a geometrical edge barrier and bulk pinning upon the magnetic field dependence of I_c for type-II superconducting strips. We shall show how the dependence of I_c upon H_a is controlled by the parameter $p = I_p/I_{s0}$, where I_p is the bulk-pinning critical current in the absence of a geometrical edge barrier, and I_{s0} is the geometrical-barrier critical current in the absence of bulk pinning.

We consider a superconducting strip of thickness d ($|y| < d/2$) and width $2W$ ($|x| < W$) centered on the z axis. We assume that d is less than the London penetration depth λ and that W is much larger than the two-dimensional screening length $\Lambda = 2\lambda^2/d$. The strip is subjected to a perpendicular applied magnetic field $\mathbf{H}_a = (0, H_a, 0)$, and it carries a total current I in the z direction described by a spatially dependent sheet current density $\mathbf{K}(x) = \mathbf{J}d = [0, 0, K_z(x)]$. We wish to determine the current-density and magnetic-field distributions at the critical current at which a steady-state flux-flow voltage appears along the length of the strip. For a strip containing no magnetic flux, $K_z(x)$ is the sum of two contributions,⁸

$$K_{Iz}(x) = \frac{I}{\pi\sqrt{W^2 - x^2}}, \quad (1)$$

the Meissner-state current density generated by the applied current I , and

$$K_{az}(x) = \frac{2H_ax}{\sqrt{W^2 - x^2}}, \quad (2)$$

the Meissner-state current density induced by the applied field H_a . The divergences in Eqs. (1) and (2) at $|x| = W$ are cut off when x is within Λ of the edge.

To account for the edge barrier, we assume that vortices nucleate and enter the superconductor when K_z at either sample edge reaches the value $K_s = j_s d$ at which the barrier is overcome. For an ideal edge, j_s is equal to the Ginzburg-Landau depairing current density j_{GL} ^{18,19}, but for an extremely defected edge, j_s may become negligibly small. When $H_a = 0$, the sheet current at both edges is approximately $K_{Iz} \approx I/\pi\sqrt{2W\Lambda}$, such that the edge-barrier critical current in zero external magnetic field is $I_{s0} \approx \pi K_s \sqrt{2W\Lambda}$. When $H_a > 0$, the net sheet current at $x = W$ is approximately $K_z \approx (I + 2\pi H_a W)/(\pi\sqrt{2W\Lambda})$, and the edge-barrier critical current becomes $I_s(H_a)/I_{s0} = 1 - h$ for small h , where $h = H_a/(I_{s0}/2\pi W)$. This result is essentially the same as that found in Ref.⁸ for the critical current in low applied magnetic fields for bulk-pinning-free strips.

We next account for bulk pinning, characterized via a bulk-pinning critical sheet current density, $K_p = j_p d$, such that the critical current in the absence of an edge barrier is $I_p = 2K_p W$. We first consider the case of relatively weak bulk pinning when $I_p < (2/\pi)I_{s0}$, i.e., $p < 2/\pi$. In low fields ($0 < H_a < H_d$, region I of Fig. 1), vortices nucleate on the right-hand side at $x = W$ when I slightly exceeds $I_s(H)$. As long as $K_z(x) = K_{Iz}(x) + K_{az}(x)$ exceeds K_p , these vortices are driven entirely across the strip, traveling rapidly (speed v governed solely by the force-balance equation $[K_z(x) - K_p]\phi_0 = \eta v d$, where η is the viscous drag coefficient), and annihilating with their images on the opposite side of the strip. The critical current is then $I_c(H_a, p) = I_s(H_a)$, and the normalized critical current is

$$i_c(h, p) = I_c(H_a, p)/I_{s0} = 1 - h. \quad (3)$$

However, K_{min} , the minimum value of $K_z(x)$, decreases with increasing H_a and reaches K_p at $I = I_s(H_a)$ when $H_a = H_d$, where

$$h_d = H_d / (I_{s0} / 2\pi W) = \frac{1}{2} [1 - (\pi p / 2)^2]. \quad (4)$$

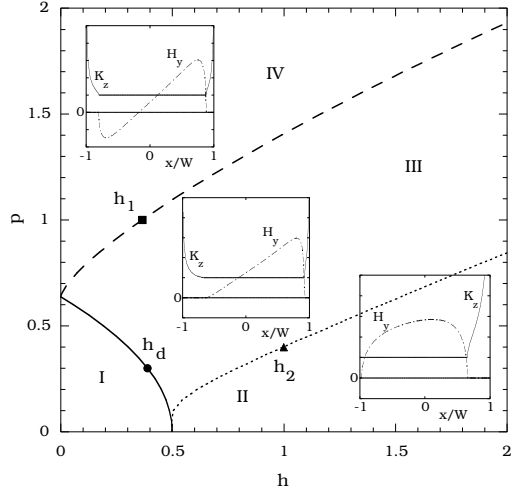


FIG. 1. Behavior at the critical current vs reduced field h and bulk pinning parameter p . In region I, the strip is vortex-free [$H_y(x, 0) = 0$] and the sheet current density is everywhere above the bulk-pinning critical value [$K_z(x) > K_p$]. In II, there is a vortex-free zone where $K_z(x) > K_p$ on the right side of the strip and a vortex dome (dot-dashed curve in inset) where $K_z(x) = K_p$ (solid curve in inset). In III, there are three zones: two vortex-free zones on either side of a vortex dome. In IV, there are four zones: a vortex dome where $H_y(x, 0) > 0$, an antivortex dome where $H_y(x, 0) < 0$, and two vortex-free zones where $K_z(x) > K_p$ near the edges. The curve $h_d(p)$ (solid) separates regions I and III, $h_1(p)$ (dashed) separates III and IV, and $h_2(p)$ (dotted) separates II and III.

When $p < 2/\pi$ and $h > h_d$ or when $p > 2/\pi$, i.e., for h and p outside region I of Fig. 1, nucleated vortices stop inside the strip, and dome-like flux distributions occur at the critical current. To determine the critical current with domes present, one must first calculate the vortex (and antivortex) density $n(x) = \mu_0 H_y(x, 0) / \phi_0$ inside the dome, where $K_z(x) = K_p$, and the sheet current density $K_z(x)$ outside, where $n(x) = 0$. We have obtained these mathematically by using the Cauchy integral inversion method^{12,4,7,9,20} to invert the Biot-Savart law. However, we shall use the method of complex fields²¹ to give a physical interpretation of the mathematical results.

Following Ref.²¹, we express the two-dimensional field distribution as an analytic function $H(\zeta) = H_y(x, y) + iH_x(x, y)$ of the complex variable $\zeta = x + iy$, such that the Biot-Savart law becomes

$$H(\zeta) = H_a + \frac{1}{2\pi} \int_{-W}^W \frac{K_z(u)}{\zeta - u} du. \quad (5)$$

The inversion procedure yields $H(\zeta)$ of the following form at the critical current $I_c(H_a)$:

$$H(\zeta) = \frac{(\zeta - a)^{1/2}(\zeta - b)^{1/2}}{(\zeta^2 - W^2)^{1/2}} [H_a + \frac{K_p}{2\pi} Q(a, b, \zeta)], \quad (6)$$

where

$$Q(a, b, \zeta) = \int_a^b \frac{\sqrt{W^2 - u^2}}{(\zeta - u)\sqrt{(u - a)(b - u)}} du \quad (7a)$$

$$= \frac{2(W + a)}{\sqrt{(W - a)(W + b)}} \left[\frac{(W - \zeta)}{(\zeta - a)} \mathbf{\Pi} \left(\frac{(\zeta + W)(b - a)}{(\zeta - a)(W + b)}, q \right) + \mathbf{\Pi} \left(\frac{b - a}{W + b}, q \right) \right], \quad (7b)$$

and

$$q^2 = \frac{2W(b - a)}{(W - a)(W + b)}. \quad (8)$$

In Eq. (6), the term proportional to H_a is simply the complex field describing the Meissner-state response to the applied field H_a of two parallel superconducting strips^{8,22} ($-W < x < a$ and $b < x < W$). The term proportional to K_p is the complex field describing the image-current response²³ of the two strips to currents $K_p du$ summed over the region $a < u < b$. We have evaluated the integral in Eq. (7a) in terms of complete elliptic integrals of the third kind²⁴⁻²⁸ $\mathbf{\Pi}(n, k)$, where n is called either the characteristic or the parameter, and k is called the modulus. Equation (7b) can be used to evaluate $H_y(x, 0) = \text{Re}H(x)$ and $K_z(x) = -2\text{Im}H(x + i\epsilon)$.

For $p > 2/\pi$ and small values of h , i.e., for h and p in region IV of Fig. 1, the vortex distribution at the critical current can be described as a double dome, consisting of a vortex dome adjacent to an antivortex dome (see inset). Just above the critical current, vortices nucleate at $x = W$ ($x' = 1$), where $K_z(W - \Lambda) = K_s$, move rapidly to the left through an otherwise vortex-free region ($b < x < W$), and then move slowly to the left through a vortex-filled region (the vortex dome), $a_+ < x < b$. Antivortices nucleate at $x = -W$, where $K_z(-W + \Lambda) = K_s$, move rapidly to the right through an otherwise vortex-free region ($-W < x < a$), and then move slowly to the right through an antivortex-filled region (the antivortex dome), $a < x < b_-$. Vortices and antivortices annihilate where the two domes meet at $x = b_- = a_+$.

Two equations must be solved simultaneously for a and b at the critical current $I_c(H_a)$ for known values of h and p in region IV of Fig. 1. One condition is that $K_z(W - \Lambda) = K_s$, which yields from Eqs. (6) and (7b)

$$\sqrt{(1 - a')(1 - b')}h + (1 + a')\sqrt{\frac{1 - b'}{1 + b'}} \mathbf{\Pi} \left(\frac{b' - a'}{1 + b'}, q \right) p = 1, \quad (9)$$

where we use the normalized quantities $a' = a/W$ and $b' = b/W$. The other condition, that $K_z(-W + \Lambda) = K_s$, yields

$$-\sqrt{(1+a')(1+b')}h + (1-b')\sqrt{\frac{1+a'}{1-a'}}\mathbf{\Pi}\left(\frac{b'-a'}{1-a'}, q\right)p = 1. \quad (10)$$

Expansion of Eq. (5) for large ζ yields $H(\zeta) = H_a + I/2\pi\zeta + \mathcal{O}(1/\zeta^2)$. Expanding Eqs. (6) and (7a) in powers of ζ and making use of Eq. (9), we obtain the normalized critical current, $i_c = I_c/I_{s0}$:

$$i_c(h, p) = -\frac{a'+b'}{2\sqrt{(1-a')(1-b')}} + \frac{1}{2}\sqrt{\frac{1+b'}{1-a'}}[(1-a')\mathbf{E}(q) + (1+a')\mathbf{K}(q)]p, \quad (11)$$

where a' and b' are determined from Eqs. (9) and (10) for the desired values of h and p .

The double-dome vortex-antivortex distribution (region IV of Fig. 1) occurs at i_c only for h in the range $0 < h < h_1$ for $p > 2/\pi$. Here, $h_1(p)$ is the lowest value of h that makes $H_y(x, 0) > 0$ in the region $a < x < b$. Thus, one of the equations determining h_1 is $H_a + (K_p/2\pi)Q(a, b, a + \epsilon) = 0$ [see Eq. (6)], which yields

$$h + \frac{1}{(b'-a')\sqrt{(1-a')(1+b')}} [(1-a')(1+b')\mathbf{E}(q) - (1+a')(1-b')\mathbf{K}(q) - (b'-a')(1-b')\mathbf{\Pi}\left(\frac{b'-a'}{1-a'}, q\right)]p = 0. \quad (12)$$

h_1 can be determined for a given value of p as the value of h when Eqs. (9), (10), and (12) are simultaneously solved for a' , b' , and h .

For known values of h and p in region III of Fig. 1, the left and right boundaries of the vortex dome a' and b' are determined by simultaneously solving Eqs. (9) and (12); Eq. (12) also gives the condition that $dK_z(x)/dx = 0$ at $x = a$. Once a' and b' are found, Eq. (11) again can be used to calculate the critical current. Just above the critical current, vortices nucleate at $x = W$, move rapidly to the left through the vortex-free region $b < x < W$, move slowly to the left through the vortex dome $a < x < b$, escape from the dome, and finally move rapidly to the left through the vortex-free region $-W < x < a$.

For increasing values of h , the left boundary of the vortex-filled region moves closer to the left edge of the strip; a becomes equal to $-W + \Lambda$ when $h = h_2$, which can be determined for a given value of p as the value of h when Eqs. (9) and (12) are numerically solved for b' and h , taking $a' = -1 + \Lambda/W$. (For Figs. 1 and 2, $\Lambda/W = 0.01$ was assumed.) For $h > h_2$, the field and current distributions and i_c can be calculated with good accuracy by simply setting $a = W$ in Eq. (6). The complex field in region II of Fig. 1 is then

$$H_{II}(\zeta) = \frac{(\zeta - b)^{1/2}}{(\zeta - W)^{1/2}} \left[H_a + \frac{K_p}{2\pi} Q(b, \zeta) \right], \quad (13)$$

where

$$Q(b, \zeta) = \int_a^b \frac{\sqrt{W-u}}{(\zeta-u)\sqrt{b-u}} du \quad (14a)$$

$$= 2 \sinh^{-1} \sqrt{\frac{W+b}{W-b}} - 2 \sinh^{-1} \sqrt{\frac{(W+b)(\zeta-W)}{(W-b)(\zeta+W)}}. \quad (14b)$$

The condition $K_z(W - \Lambda) = K_s$, which determines $b' = b/W$ at I_c for h and p in region II of Fig. 1, becomes

$$\sqrt{2(1-b')} [h + p \sinh^{-1} \sqrt{(1+b')/(1-b')}] = 1 \quad (15)$$

instead of Eq. (9), and the normalized critical current can be expressed as

$$i_c(h, p) = \frac{1}{4} \sqrt{2(1-b')} + \frac{p}{2} \sqrt{2(1+b')} \quad (16)$$

instead of Eq. (11).

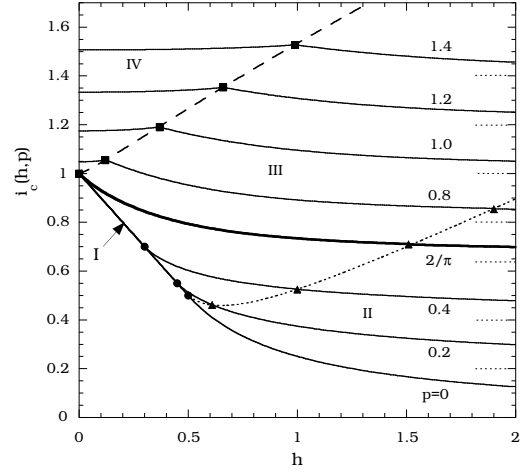


FIG. 2. $i_c(h, p)$ (critical current normalized to I_{s0}) vs reduced field h for fixed values of the bulk pinning parameter p . The solid straight line and solid circles denote values of i_c in region I, where $h = h_d(p)$; the dashed curve and solid squares show i_c at $h = h_1(p)$; and the dotted curve and solid triangles show i_c at $h = h_2(p)$. For $p < 2/\pi$, i_c decreases linearly with h [Eq. (3)] up to h_d and then decreases more slowly in regions III [Eq. (11)] and II [Eq. (16)]. The bold curve shows i_c for the special case of $p = 2/\pi$. For $p > 2/\pi$, i_c increases by a few percent in the double-dome region IV and then decreases more gradually in regions III and II. In all cases, i_c asymptotically approaches p for large h (short dotted lines along the right side of the figure).

The reduced critical current i_c as a function of h , calculated from Eq. (11) or (16), is shown in Fig. 2 for various values of p . For $p = 0$ and $h > 1/2$, we find $i_c = 1/4h$, as obtained in^{6,8} for pin-free strips with an edge barrier. In the opposite limit, $p \gg 1$, we obtain $i_c \approx p$, as expected for bulk-pinning-dominated behavior. For $h \gg p$, we see from Eq. (15) that b' approaches 1, and Eq. (16) yields $i_c \approx p + 1/4h$. A generic feature of Fig. 2 is the plateau in i_c vs h to the left of the dashed curve in region IV; actually, i_c increases by a few percent as h increases from 0 to h_1 . This increase is due to a significant decrease in the width $b - a$ over which $K_z(x)$ is restricted to K_p . This effect is partially compensated by a change in shape of

$K_z(x)$ in the vortex-free zones [e.g., $dK_z(x)/dx = 0$ at $x = a$ at $h = h_1$]. Field-dependent critical current densities $j_c(H_a)$ have been found experimentally in Refs.^{10–14}, but the behavior was interpreted solely in terms of bulk pinning.

In agreement with earlier work,^{9,29} our results show that the critical current of a strip is not a simple superposition of currents I_s and I_p , as was suggested in Refs.^{16,30,31}. Only in the limit $h \gg p$ is it possible to express the critical current as $I_c(H_a) = I_p + I_s(H_a)$.

We have assumed here that K_p is a constant. Because of the nonlocal current-field relation [Eq. (5)], it would be a challenging task to find $I_c(H_a)$ when K_p depends upon the local magnetic field $H_y(x, 0)$.

In summary, we have solved for the field dependence of the critical current density in a superconducting strip accounting for both bulk pinning and a geometrical edge barrier, and we have developed a procedure for finding the magnetic-field and current-density distributions inside the strip at the critical current. In the presence of a strong edge barrier, we have found strong field dependencies of the critical current. Such effects should be taken into account when interpreting experimental critical currents in low and moderate magnetic fields.

We thank Y. Mawatari for stimulating discussions. This work was funded by the Basic Research Foundation of Russia through Grant No. 01-02-16593, the Education Ministry (Grant No. E00-3.4-331) and the Science Ministry (Project 107-1(00)-P) of the Russian Federation, by Iowa State University of Science and Technology under Contract No. W-7405-ENG-82 with the U.S. Department of Energy, and by the National Academy of Sciences under the Collaboration in Basic Science and Engineering Program supported by Contract No. INT-0002341 from the National Science Foundation.³²

¹ E. Zeldov, A. I. Larkin, V. B. Geshkenbein, M. Konczykowski, D. Majer, B. Khaykovich, V. M. Vinokur, and H. Shtrikman, Phys. Rev. Lett, **73**, 1428 (1994).

² I. L. Maksimov and A. A. Elistratov, JETP Lett. **61**, 208 (1995).

³ M. Benkraouda and J. R. Clem, Phys. Rev. B **53**, 5716 (1996).

⁴ I. L. Maksimov and A. A. Elistratov, Appl. Phys. Lett. **72**, 1650 (1998).

⁵ A. A. Elistratov and I. L. Maksimov, Phys. Solid State **42**, 201 (2000).

⁶ M. Yu. Kupriyanov and K. K. Likharev, Fiz. Tverd. Tela **16**, 2829 (1974) (Sov. Phys. Solid State **16**, 1835 (1975)).

⁷ I. L. Maksimov, Europhys. Lett. **32**, 753 (1995).

⁸ M. Benkraouda and J. R. Clem, Phys. Rev. B **58**, 15103 (1998).

⁹ I. L. Maksimov and A. A. Elistratov, Appl. Phys. Lett. **72**, 1650 (2002).

¹⁰ A. Weyers, H. Kliem, J. Lutzner and G. Arit, J. Appl. Phys. **71**, 5089 (1992).

¹¹ K. H. Muller, D. N. Matthews, R. Driver, Physica C **191**, 319 (1992).

¹² M. Aubin and P. Fournier, Physica C **235-240**, 3081 (1994).

¹³ S. de Brion, W. R. White, A. Kapitulnik, and M. R. Beasley, Phys. Rev. B **49**, 12030 (1994).

¹⁴ F. Lefloch, C. Hoffman, and O. Demolliens, Physica C **319**, 258 (1999).

¹⁵ V. P. Andrackii, L. M. Grundel, V. N. Gubankov, and N. V. Pavlov, Zh. Eksp. Teor. Phys. **65**, 1591 (1973).

¹⁶ L. Burlachkov, A. E. Koshelev, and V. M. Vinokur, Phys. Rev. B **54**, 6750 (1996).

¹⁷ J. R. Clem, R. P. Huebener, and D. E. Gallus, J. Low Temp. Phys. **12**, 449 (1973).

¹⁸ L. G. Aslamazov, S. V. Lempickii, Zh. Eksp. Teor. Phys. **84**, 2216 (1983).

¹⁹ D. Yu. Vodolazov, I. L. Maksimov, and E. H. Brandt, Europhys. Lett. **48**, 313 (1999).

²⁰ F. D. Gakhov, *Boundary Value Problems, 2nd Edition*, English translation edited by I. N. Sneddon, (Pergamon Press, Oxford, 1966).

²¹ Y. Mawatari and J. R. Clem, Phys. Rev. Lett. **86**, 2870 (2001).

²² A. A. Babaei Brojeny, Y. Mawatari, M. Benkraouda, and J. R. Clem, Supercond. Sci. Technol.

²³ W. T. Norris, J. Phys. D **3**, 489 (1970).

²⁴ I. S. Gradshteyn and I. M. Ryzhik, *Table of Integrals, Series, and Products, 6th Edition*, edited by A. Jeffrey and D. Zwillinger (Academic Press, San Diego, 2000).

²⁵ *Handbook of Mathematical Functions*, edited by M. Abramowitz and I. A. Stegun (National Bureau of Standards, Washington, 1967).

²⁶ *Mathematica, Version 4.1*, Wolfram Research, Inc., Champaign, IL (2000).

²⁷ R. B. Selfridge and J. E. Maxfield, *A Table of the Incomplete Elliptic Integrals of the Third Kind* (Dover, New York, 1958).

²⁸ P. F. Byrd and M. D. Friedman, *Handbook of Elliptic Integrals for Engineers and Physicists* (Springer, Berlin, 1954).

²⁹ G. M. Maksimova, N. V. Zhelezina, and I. L. Maksimov, Europhys. Lett. **53**, 639 (2001).

³⁰ S. Tahara, S. M. Anlage, J. Halbritter, C.-B. Eom, D. K. Fork, T. H. Geballe, M. R. Beasley, Phys. Rev. B **41**, 11203 (1990).

³¹ Y. Paltiel, D. T. Fuchs, E. Zeldov, Y. N. Myasoedov, H. Shtrikman, M. L. Rappaport, and E. Y. Andrei, Phys. Rev. B **58**, R14763 (1998).

³² The United States Government retains and the publisher, by accepting the article for publication, acknowledges that the United States Government retains a nonexclusive, paid-up, irrevocable, world-wide license to publish or reproduce the published form of this manuscript, or allow others to do so, for United States Government purposes. The contents of this publication do not necessarily reflect the views of the National Academy of Sciences or the National Science Foundation.